Dicle University Journal of Engineering (DUJE)

web: http://dergipark.gov.tr/dumf

Research Article

Neutron and Ion Production with Various Applied Voltages in Spherical Plasma Focus

Yasar Ay [1,*]

[1] Dicle University, Faculty of Engineering, Department of Electrical and Electronics Engineering, ORCID: 0000-0002-9888-8700

ARTICLE INFO

Article history:

Received 29 January 2020
Received in revised form 11 March 2020
Accepted 12 March 2020
Available online 30 March 2020

Keywords:

Ion, Neutron, Plasma Focus, Radiation, Voltage

Doi: 10.24012/dumf.681853

ABSTRACT

In this work, the applied voltage effect on neutron yield and ion production are studied by varying the charging voltage between 15 kV and 30 kV with 1 kV increment to investigate neutron yield, radiation emissions and ion properties using the developed MHD model. While Joule heating, radiative recombination, bremsstrahlung and line radiation are calculated as radiation terms, beam-ion speed, energy and density are calculated as ion properties. The dominant neutron production mechanism is beam-target which results from the accelerated energetic ions under the diode voltage which is calculated along with neutron yield. In this study, while maximum neutron yield is 2.63 10^{13} for 30 kV charging voltage, beam-ion energy and speed reach 61 keV and 240 cm/μs, respectively.

* Corresponding author
Yasar, Ay
✉ yasar.ay@dicle.edu.tr

Please cite this article in press as Y. Ay, "Neutron and Ion Production with Various Applied Voltages in Spherical Plasma Focus", DUJE, vol. 11, no.1, pp. 135-141, March 2020

Introduction

Hot and dense plasma sources can be produced by the gas discharge of the pulsed plasma focus (PF) devices. The geometry of PF devices is mostly cylindrical, which are named as "Mather type" or "Filippov type" PF devices. These devices mainly have different electrode configurations. Spherical plasma focus (SPF) as a new design is used in this study. The PF devices can accelerate the beams of electrons and ions to high energies for neutron, x-rays and energetic ion production by using deuterium (D), Tritium (T) or a mixture of both gases (DT).

Thermonuclear and beam-target are the two ways of producing neutrons in PF. [1]. Beam target is the main neutron production in SPF. While the beam-target neutrons result from the interaction of the plasma with the accelerated beam-ions under diode voltage, thermonuclear neutrons are generated with interaction of deuterons in radiative phase of the plasma focus devices [2].

Neutron production is one of important aspects of PF investigations. Therefore, investigating the ways of increasing neutron yield from the PF devices are studied in terms of capacitor bank energy [3], gas pressure [4], and energy transformation [5]. All of these parameters have strong effect on neutron yield in PF devices. Neutron yield is also influenced by anode properties of PF such that neutron yield can be increased by using a hollow anode [6], a conical tip on anode [7], and a converging anode shape [8] in PF device. In addition to the effect of the anode shape on the neutron yield, it also has a strong effect on x-ray emissions. Comparing two anode shapes (converging anode and conventional cylindrical anode) for neutron yield and x-ray emission shows that while cylindrical anode leads to higher neutron yield, x-ray emission is higher for converging anode. Even though neutron yield is lower when converging anode is used in the plasma focus device, neutron energy is higher when using converging anode shape [8].

Different anode tips were investigated in the PF device for soft x-ray production by Habibi and Mahtab [9]. Cylindrical-flat, cylindrical-hollow, spherical-convex, cone-flat, and cone-hollow anode tips were used with the plasma focus device. While using cone-flat, spherical-convex, and cone-hollow anode tips resulted in a significant increase in x-ray intensity compared with conventional cylindrical-flat anode tips, using cylindrical-hollow tip showed a decrease in x-ray intensity. In this study, cone-flat anode produced the highest x-ray intensity. Therefore, it can be used to optimize PF as an x-ray source.

While soft x-rays are originated from the plasma itself, hard x-rays result from the interaction of the electron beams with anode. Since soft x-ray and hard x-ray emission have different production mechanisms in the PF devices, they also have different optimum operating conditions. Therefore, PF devices can be optimized for either soft x-ray emission or hard x-ray emission even though increasing charging voltage increases both soft x-ray and hard x-ray emissions, which shows that x-ray production has a strong correlation with charging voltage in the cylindrical plasma focus devices [10].

An MHD model for SPF is developed and validated [11,12], SPF is optimized for neutron production [13] and the effect of the various cathode radius on the plasma dynamics is investigated [14] in the previous works.

This work investigate the effect of the charging voltage on neutron and ion production, and radiation emissions in SPF by using MHD model to simulate SPF. In addition to the calculation of the ion properties (speed, energy and density) in the SPF, neutron yield, Joule heating, bremsstrahlung radiation, radiative recombination and line radiation are also investigated with respect to charging voltage variation. In this study, the charging voltage variation is between 15 kV and 30 kV with 1 kV increment for each calculation step for the above-mentioned investigations.

Spherical Plasma Focus Model

A model for SPF has been developed and validated. The detailed theory of the model with

the derivation of the equations and validation of the model were explained in detail in the previous works [11,12].

The model consists of 4 phases: rundown phase I, rundown phase II, reflected shock phase and radiative phase. In the model, the snowplow model and shock wave equations and equivalent circuit equations are used to describe SPF. Figure 1 shows SPF device and the equivalent circuit. In the circuit model, V_0 : charging voltage, C_0 : capacitor bank, L_0 : circuit inductance, r_0: circuit resistance, L_p : plasma inductance, r_p : plasma resistance.

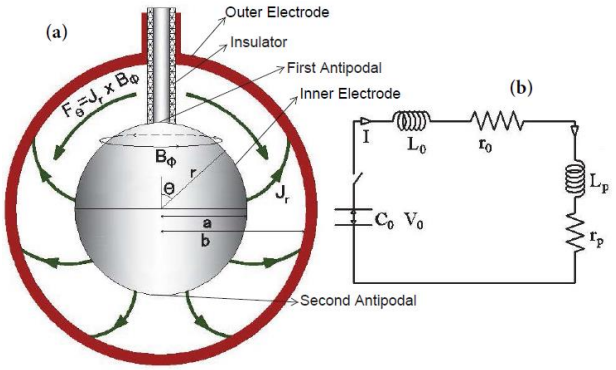

Figure 1. (a) SPF device. (b) Equivalent circuit model

The plasma focus devices produce high density-high temperature plasma which is called pinch. The CS is formed by electrical discharge and accelerated as the first step for pinch production (rundown phase I), and then it is compressed after the current sheath passes the equator point of SPF device (rundown phase II). Since CS is supersonic, an ionizing shock wave is formed in front of CS. After the shock front hits the axis of the SPF device, it is reflected and starts moving to CS (reflected shock phase), to produce the high density-high temperature pinch (radiative phase).

Starting point for rundown phase I is CS formation and this phase finishes when CS reaches the equator of SPF which is the beginning of the rundown phase II. Rundown phase II ends and reflected shock phase starts when the shock front hits the axis of the SPF device. Then shock front moves towards the coming CS until the reflected shock front and the coming CS meet, that is the end of the reflected shock phase and the beginning of the radiative phase. Compression of plasma continues in radiative phase which ends at the maximum compression with the plasma disruption.

Governing Equations

Derivation of the equations is given in the previous works [11, 12]. Therefore, only the final equations are given here.

Since CS changes momentum because of the magnetic pressure on the CS, The change in the momentum is set equal to the magnetic pressure and this equation is solved to find equation of motion for CS as follows for all phases [11,12].

Equation of motion for rundown phase I:

$$\ddot{\theta} = \frac{\alpha^2 I^2}{r sin\theta\ (cos\theta_0 - cos\theta)} - \frac{\dot{\theta}^2 sin\theta}{cos\theta_0 - cos\theta}$$

Equation of motion for rundown phase II and reflected phase:

$$\ddot{\theta} = \frac{\alpha^2 I^2}{r cos(\theta - \pi/2)(cos\theta_0 - cos\theta)} - \frac{\dot{\theta}^2 sin\theta}{cos\theta_0 - cos\theta}$$

where $\alpha = \frac{3\mu_0 f_c^2 \ln\left(\frac{b}{a}\right)}{8\pi^2 \rho f_m (b^3 - a^3)}$ is a scaling parameters that consist of constant values. I is discharge current, r is the distance for plasma parameter calculations, θ is angle of the motion, θ_0 is an angle corresponding to the insulator volume, μ_0 is permeability of free space, f_c and f_m are current and mass fraction, a is inner and b is outer electrode radius, ρ represents initial gas density.

For the last phase (radiative phase), radiation terms are taken into account and there is third force on the CS due to radiation emissions. In this phase, the momentum change of the current sheath is because of the magnetic pressure on the current sheath and radiation emission, which leads to the following equation as the equation of the motion for radiative phase.

$$\ddot{\theta} = \frac{\alpha^2 I^2}{r cos(\theta - \pi/2)} - \frac{sin\theta\ \dot{\theta}^2}{C} - \frac{3QA}{2\pi\rho f_m (b^3 - a^3) r C}$$

Where $C = cos\theta_0 - cos\theta$ and A is plasma column surface area.

Equation for neutron yield:

$$Y = N_b N_i V_{col} \sigma v_b$$

Where N_b and N_i are beam-ion number density and plasma-ion number density, V_{col} is the pinch volume, σ is cross section for DT reaction, v_b is beam-ion velocity.

Plasma-ion number density:

$$N_i = N_0 f_m \frac{2}{1 + cos\theta}$$

Beam-ion number density:

$$N_b = \frac{f_i L\, I^2 f_c^2}{2eUV_{col}}$$

Where N_0 is ambient gas number density, e is the elementary charge, and U is diode voltage.

Results and Discussion

Concentric spherical plasma focus device with 432 μF capacitor bank energy, 14.5 Torr pressure (equal amount of D-T gas mixture), and 36 nH external inductance is used in this study to investigate effect of charging voltage on neutron yield, x-rays and ion properties. The inner and outer electrode radii of SPF are 8 cm and 14.5 cm. 15-30 kV charging voltage range with 1 kV increment is used and maximum values of the investigated parameters with respect to charging voltage are given.

Figure 2 shows the maximum beam-target neutron yield for each charging voltage. While neutron yield for 15 kV charging voltage is 1.48 x 10^{11} neutron, it is rapidly increasing to 2.63 x 10^{13} neutron for 30 kV charging voltage due to the increasing beam-ion speed (Figure 5) under diode voltage (Figure 3).

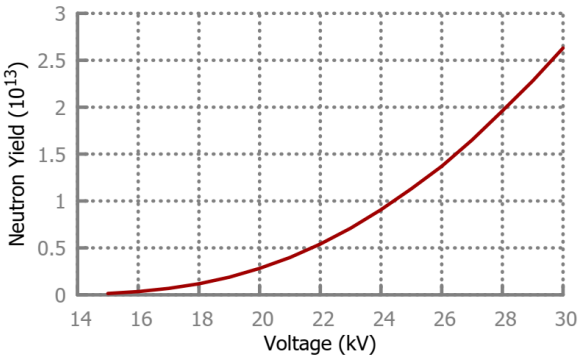

Figure 2. Beam-Target Neutron Yield

While Figure 3 shows the maximum diode voltage, which occurs due to the plasma disruption, with respect to charging voltage, Figure 4 and Figure 5 show the maximum beam-ion energy for each voltage and the corresponding maximum speed of the beam-ions which are accelerated under diode voltage and the interaction of these ions with plasma produces beam-target neutrons.

Maximum diode voltage is 15 kV for 15 kV charging voltage and it quadruples to 60 kV for 30 kV charging voltage. Since beam-ions are accelerated under this diode voltage with a speed proportional to square root of the beam-ion energy, maximum speed of beam-ions are doubled while changing charging voltage from 15 kV to 30 kV. Beam-ion speed reaches the maximum of 240 cm/μs for 30 kV charging voltage and the corresponding maximum beam-ion energy is rapidly increasing from 15 keV to 61 keV while varying the charging voltage from 15 kV to 30 kV.

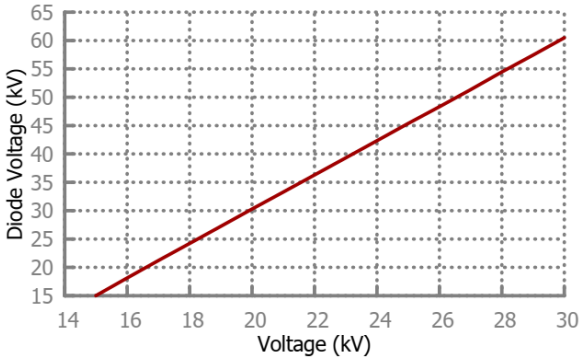

Figure 3. Diode Voltage

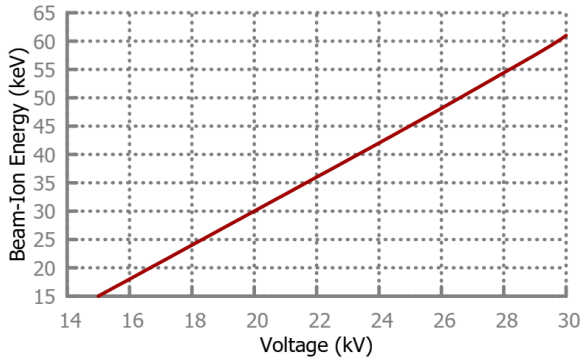

Figure 4. Beam-Ion Energy

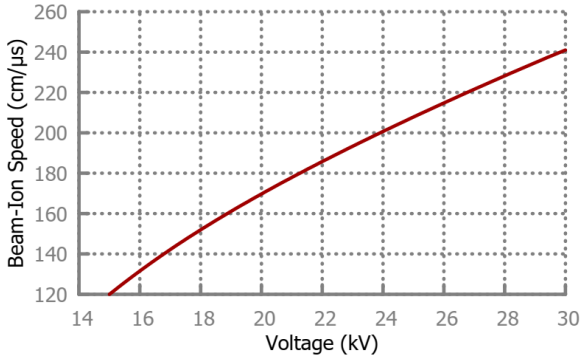

Figure 5. Beam-Ion Speed

Figure 6 shows the maximum beam-ion density for each charging voltage. Increasing charging voltage results in a decrease in maximum beam-ion density. Max beam-ion density is 7.66 x 10^{20} m^{-3} for 15 kV charging voltage and it decreases to 6.82 x 10^{20} m^{-3} for 30 kV charging voltage.

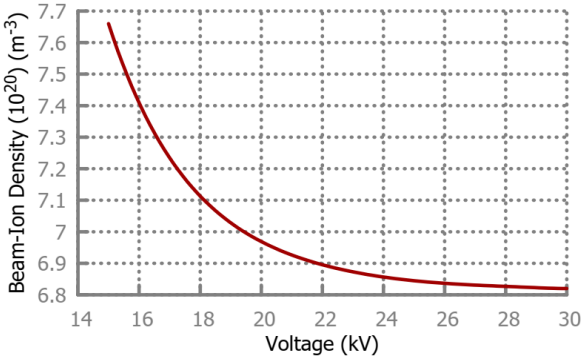

Figure 6. Beam-Ion Density

The temperature of plasma in radiative phase is shown in Figure 7. In this figure, while "Max T" represents the maximum temperature that the plasma can reach in this phase for each charging voltage, "Min T" represents the minumum temperature of the plasma for each charging voltage. While max plasma temperature is 8.45 eV for 15 kV charging voltage and increases to 29.1 eV for 30 kV charging voltage, minimum plasma temperature is 5.06 eV for 15 kV charging voltage and increases to 18.14 eV for 30 kV charging voltage. Changing charging voltage from 15 kV to 30 kV increases maximum and minimum plasma temperatures but it also increases the difference between maximum and minimum plasma temperatures, which shows that plasma column loses more energy through radiation emissions for higher charging voltages in radiative phase.

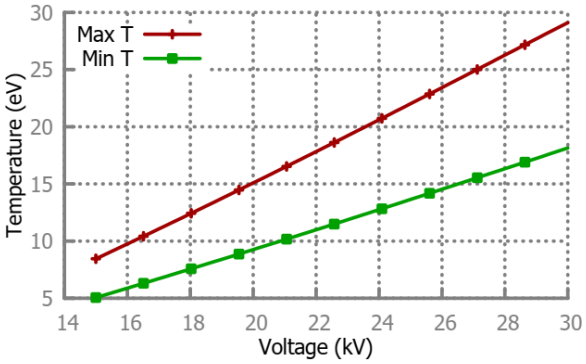

Figure 7. Plasma Temperature

While Figure 8 shows the maximum power densities for Joule heating (PJ), bremsstrahlung radiation (PBR) and line radiation (PLN), Figure 9 shows the maximum power density for radiative recombination (PREC).

The plasma energy in radiative phase is mainly influenced by power densities such that Joule heating increases the plasma energy but bremsstrahlung and line radiation, and radiative recombination decrease the energy of the plasma in this phase. In this study, radiative recombination effect is on the order of 10^8. The effect of the Joule heating, bremsstrahlung and line radiations are on the order of 10^{11}. Max power density for radiative recombination is 1.1 x 10^8 W/m^3 for 15 kV charging voltage and it increases to 2.1 x 10^8 W/m^3 for 30 kV charging voltage. Varying charging voltage from 15 kV to 30 kV results in decreasing maximum Joule heating for each charging voltage from 4.4 x 10^{11} to 2.3 x 10^{11} W/m^3 but it increases the maximum

bremsstrahlung radiation (from 0.9 x 10^{11} to 1.8 x 10^{11} W/m^3) and line radiation (from 0.7 x 10^{11} to 5.1 x 10^{11} W/m^3) power densities.

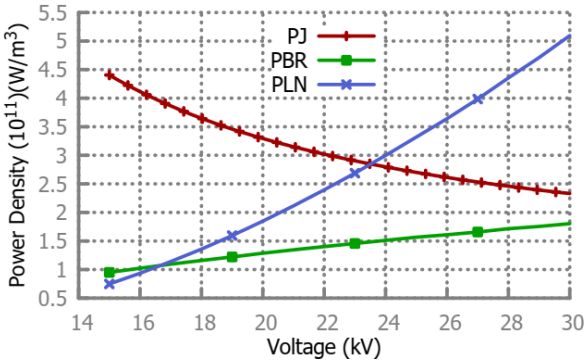

Figure 8. Joule heating, bremsstrahlung and line radiation power densities

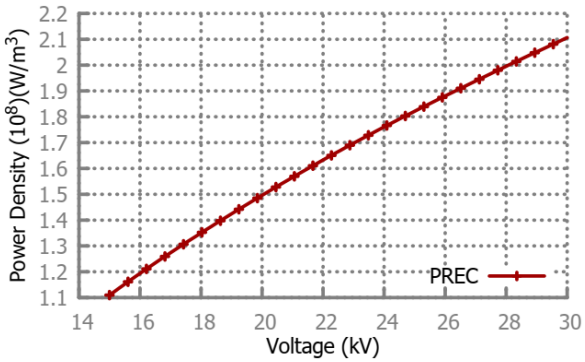

Figure 9. Radiative recombination power density

Conclusions

In this study, the main focus is to investigate the charging voltage variation effect on SPF. For that reason, maximum radiation power densities (Joule heating, bremsstrahlung and line radiation, and radiative recombination), maximum ion properties (beam-ion speed, energy, and density) and maximum neutron yields are calculated in SPF. Increasing the charging voltage results in increasing the maximum beam-ion speed and energy but decreases the maximum beam-ion density. Beam-ion energy and speed reach 61 keV and 240 cm/μs for 30 kV charging voltage and maximum beam-ion density is decreasing from 7.66 x 10^{20} m^{-3} to 6.82 x 10^{20} m^{-3} while changing charging voltage from 15 kV to 30 kV with 1 kV increment. This voltage variation has also significant effect on the radiation power densities such that the increase in charging voltage results in decreasing maximum Joule heating that is the mechanism for the plasma to gain energy but it increases the maximum line and bremsstrahlung radiation, and radiative recombination power densities which are the way of losing energy. Therefore, the spherical plasma focus is losing more energy for higher charging voltages in the radiative phase. The maximum beam-target neutron yield is also influenced by the voltage variation. Increasing the charging voltage from 15 kV to 30 kV leads to a rapid increase in neutron yield which is 1.48 x 10^{11} for 15 kV charging voltage and increased rapidly to 2.63 x 10^{13} for 30 kV charging voltage.

Acknowledgements

This work was supported by The Scientific and Technological Research Council of Turkey, Project No: 119F039

References

1. Castillo, F.; Milanese, M.; Moroso, R.; Pouzo, J. Evidence of thermal and non-thermal mechanisms coexisting in dense plasma focus d-d nuclear reactions. Journal of Physics D: Applied Physics 1999, 33 (2), 141–147.

2. Gribkov, V.A.; Banaszak, A.; Bienkowska, B.; Dubrovsky, A.V.; Ivanova-Stanik, I.; Jakubowski, L.; Karpinski, L.; Miklaszewski, R.,A.; Paduch, M.; Sadowski, M.J.; Scholz, M.; Szydlowski, A.; Tomaszewski, K. Plasma dynamics in the PF-1000 device under fullscale energy storage: II. fast electron and ion characteristics versus neutron emission parameters and gun optimization perspectives. Journal of Physics D: Applied Physics 2007, 40 (12), 3592–3607.

3. Talaei, A.; S. Kiai, S.M. Study the influence of the bank energy on the dynamical pinch in plasma focus. Journal of Fusion Energy 2009, 28 (3), 304–313.

4. Singh, A.; Sing, L.; and Saw, S.H. Effect of the variation of pressure on the dynamics and

neutron yield of plasma focus machines. IEEE Transactions on Plasma Science 2017, 45 (8), 2286–2291.

5. Kubes, P.; Klir, D.; Kravarik, J.; Rezac, K.; Paduch, M.; Pisarczyk, T.; Scholz, M.; Chodukowski, T.; Bienkowska, B.; Ivanova-Stanik, I.; Karpinski, L.; Sadowski, M.J.; Tomaszewski, K.; Zielinska, E. Energy transformations in column of plasma-focus discharges with megaampere currents. IEEE Transactions on Plasma Science 2012, 40 (2), 481–486.

6. Shaw, B.H.; Chapman, S.; Cooper, C.M.; Goyon, C.; Angus, J.; Link, A.; Higginson, D.P.; Liu, J.X.; Mitrani, J.M.; Podpaly, Y.A.; Povilus, A.; Schmidt, A. Maximizing neutron yields by scaling hollow diameter of a dense plasma focus anode. Journal of Applied Physics 2018, 124 (23), 233301.

7. Kubes, P.; Paduch, M.; Cikhardt, J.; Cikhardtova, B.; Klir, D.; Kravarik, J.; Rezac, K.; Zielinska, E.; Sadowski, M.J.; Szymaszek, A.; Tomaszewski, K.; Zaloga, D. Increase in the neutron yield from a dense plasma-focus experiment performed with a conical tip placed in the centre of the anode end. Physics of Plasmas 2017, 24 (9), 092707.

8. Talukdar, N.; Borthakur, S.; Neog, N.K.; Borthakur, T.K. Comparative study of neutron emission from a plasma focus device using two different anode shapes. Physics of Plasmas 2016, 23 (5), 052711.

9. Habibi, M.; Mahtab, M. Experimental study of soft x-ray intensity with different anode tips in amirkabir plasma focus device. Pramana 2016, 87 (1).

10. Roomi, A.; Saion, E.; Habibi, M.; Amrollahi, R.; Baghdadi, R.; Etaati, G.R.; Mahmood, W.; Iqbal, M. The effect of applied voltage and operating pressure on emitted x-ray from nitrogen (n2) gas in APF plasma focus device. Journal of Fusion Energy 2011, 30 (5), 413–420.

11. Ay, Y.; Al-Halim, M.A.; Bourham, M.A. Simulation of the plasma sheath dynamics in a spherical plasma focus, The European Physical Journal D 2015, 60 (9).

12. Ay, Y.; Al-Halim, M.A.; Bourham, M.A. MHD simulation for neutron yield, radiations and beam–ion properties in the spherical plasma focus. Journal of Fusion Energy 2015, 35 (2), 407–414.

13. Ay, Y. A neutron source with 10^{14} DT neutron yield, International Journal of Modern Physics E 2020. DOI:10.1142/S0218301319500976

14. Ay, Y. Effect of the cathode radius on plasma dynamics and radiation emissions in a spherical plasma focus device, Physics of Plasmas 2019, 26(10) 102506.